MINERALIZATION OF HETERO BI-FUNCTIONAL REACTIVE DYE IN AQUEOUS SOLUTION BY FENTON AND PHOTO-FENTON REACTIONS

Francesc Torrades[a]*, José Antonio García-Hortal[b], Julia García-Montaño[c]

[a]Departament d'Enginyeria Química, ETSEIA de Terrassa, Universitat Politècnica de Catalunya, C/Colom 11, E-08222, Terrassa (Barcelona) Spain.

E-mail: francesc.torrades@upc.edu; FAX: 34937398101; TEL: 34937398148

[b]Departament d'Enginyeria Tèxtil i Paperera, ETSEIA de Terrassa, Universitat Politècnica de Catalunya, C/Colom 11, E-08222, Terrassa (Barcelona) Spain.

E-mail: garcia.hortal@upc.edu

[c]LEITAT Technological Center, Environment R&D Department, C/Innovació, 2, E-08225 Terrassa (Barcelona), Spain.

E-mail: jgarcia@leitat.org

*To whom correspondence should be addressed

Acknowledgement

The authors thank, Polytechnic University of Catalonia (Spain), for facilities and support in doing experimental work.

ABSTRACT

This study focused on the advanced oxidation of the hetero bi-functional reactive dye Sumifix Supra Yellow 3RF (CI Reactive Yellow 145) using dark Fenton and photo-Fenton conditions in a lab-scale experiment. A 2^3 factorial design was used to evaluate the effects of the three key factors: temperature, Fe (II) and H_2O_2 concentrations, for a dye concentration of 250 $mg \cdot L^{-1}$ with chemical oxygen demand (COD) of 172 $mg \cdot L^{-1}$ O_2 at pH = 3. The response function was the COD reduction. This methodology lets us find the effects and interactions of the studied variables and their roles in the efficiency of the treatment process. In the optimization, the correlation coefficients for the model (R^2) were 0.948 and 0.965 for Fenton and photo-Fenton treatments respectively. Under optimized reaction conditions: pH = 3, temperature = 298 K, $[H_2O_2]$ = 11.765 mM and [Fe(II)] = 1.075 mM; 60 min of treatment resulted in a 79 % and 92.2 % decrease in COD, for the dye taken as the model organic compound, after Fenton and photo-Fenton treatments respectively.

Keywords: Advanced oxidation processes; central composite design; COD reduction; Fenton and photo-Fenton reactions; reactive dye

1. Introduction

The textile industry is related to discharge of large quantities of water that are highly coloured and contain high levels of organic matter [1-3]. Such pollution is associated with the use of large amounts of dyes during the dyeing stages [4]. Dyes have different organic structures with unsaturated groups that act as chromophores and gave the dye its colour.

Because of the non biodegradable nature of most of these dyes and the limitation of physical and chemical treatment techniques [5,6], new processes to treat such wastewaters have been developed. In this direction, and taking advantage of high oxidative power of the ·OH radical (2.8 V versus NHE), several treatments catalogued under the designation of advanced oxidation processes (AOPs) have been used for organic pollutant abatement. Among the different existing AOPs, we can find Fenton-based processes which have been encountering a notable development due to their favourable results in combination with easy handling [7], and can be used to the degradation of this kind of effluents [8-12]. These processes are highly effective in the effluents remediation and have a special interest and constant development [13]. Moreover, it makes possible high reactions yields associated to a low cost treatment.

In Fenton's processes, the generation of hydroxyl radicals and Fe^{2+} regeneration takes place according the following reactions (reactions 1-4):

$$Fe^{2+} + H_2O_2 \rightarrow Fe^{3+} + {}^{\bullet}OH + {}^{-}OH \qquad k = 76.5\ L\cdot mol^{-1}\cdot s^{-1} \qquad (1)$$

$$Fe^{3+} + H_2O_2 \leftrightarrow FeOOH_2^{+} + H^{+} \qquad K_{eq} = 3.10\cdot 10^{-3} \qquad (2)$$

$$FeOOH^{2+} \rightarrow HO^{\bullet}_2 + Fe^{2+} \qquad k = 2.70\cdot 10^{-3}\ s^{-1} \qquad (3)$$

$Fe^{3+} + HO^{\bullet}_2 \rightarrow Fe^{2+} + O_2 + H^+$ $k < 2.00 \cdot 10^3$ $L \cdot mol^{-1} \cdot s^{-1}$

(4)

The rate of contaminants degradation can be considerably increased when ultraviolet light is simultaneously irradiated in the photo-Fenton's process [7]. In this case, the regeneration of Fe^{2+}, with production of new $HO^{\bullet}$ radicals, follows reactions (5) and (6):

$Fe^{3+} + H_2O \rightarrow FeOH^{2+} + H^+$ (5)

$FeOH^{2+} \xrightarrow{h\upsilon} Fe^{2+} + HO\cdot$ $\lambda \leq 410$ nm (6)

Fenton processes depend on various variables that can modify the degradation of organic matter present in the sample, such as pH, temperature, source of light and the H_2O_2 and Fe^{2+} concentrations. However, in most of the literature studies on Fenton reagent treatment of dyestuffs, each variable was suited independently, with the other variables held constant. Moreover, most of these studies report decolourization efficiencies, but not COD removal or mineralization.

This high number of influential variables makes suitable using experimental design techniques. These techniques provide a systematic way of working that allows conclusions to be drawn about the variables or its combination that are most influential in the response factors, with a considerable reduction in the number of experiments. Among these techniques, the most used are the central composite design (CCD), Doehlert matrices, Box-Behnken designs and three-level full-factorial designs [14].

So far, we found in literature, several previous studies that investigated the use of statistical design of experiments to develop optimal AOPs to treat effluents that contained dyes. The degradation of Acid Blue 193 and Reactive Black 39 [15] using CCD and under photo-Fenton-like conditions, as well as the mineralization anthraquinone dye on immobilized TiO_2 nanoparticles [16] and Remazol black B mineralization by Fenton-like peroxidation [17] have been studied. On the other hand, Box-Behnken technique has been used on the degradation of several dyes, like as Direct Red 28 under Fenton and photo-Fenton conditions [18, 19].

However, we could not find in literature studies related to the oxidation of CI Reactive Yellow 145, a hetero bi-functional reactive dye for cellulosic fibres, by using the dark Fenton and photo-Fenton reactions in a lab-scale experiment based on central composite design.

In consequence, the goal of the present work has been to identify, by using response surface methodology, optimum Fenton and photo-Fenton conditions to degrade CI Reactive Yellow 145. Both processes were studied, and degradation efficiency was compared.

2. Materials and methods

2.1 Chemicals

In this study, a commercial hetero bi-functional reactive dye, Sumifix Supra Yellow 3RF (CI Reactive Yellow 145), from Sumitomo was used as received without further

purification. This dye had sulfatoethylsulfone and monochlorotriazine reactive groups. Its molecular formula is shown in Fig.1.

Appropriate dye solutions were prepared by dissolving the required amount of dye in deionised water. All deionised water was prepared using a Millipore Milli-Q system.

For the pH adjustment, we used concentrated reagent-grade H_2SO_4 and NaOH solutions (Panreac).

Iron sulphate heptahydrate ($FeSO_4 \cdot 7H_2O$, Merck 99.5%) and hydrogen peroxide (H_2O_2 Panreac 33% (w/v)) were mixed in order to generate the hydroxyl radical, $HO\cdot$.

2.2 Reactors and light sources

All Fenton and photo-Fenton experiments were carried out using a cylindrical Pyrex thermostatic cell of 150 ml capacity. The reaction mixture inside the cell, consisting of 100 ml of dye sample (250 $mg \cdot L^{-1}$) and defined amounts of H_2O_2 and Fe (II), were continuously stirred with a magnetic bar and the temperature fixed at the desired level.

When working under photo-Fenton's conditions, as artificial source of light was used a 6 W Philips black light fluorescent lamp, which basically emits at 350-400 nm. The intensity of the incident UVA light, measured using a uranyl actinometer, was 1.38 x 10^{-9} Eienstein s^{-1}.

During the experiments, aliquots were withdrawn from the solution in order to measure COD.

2.3 Analytical methods

Chemical Oxygen Demand (COD, $mg \cdot L^{-1}$ O_2) was obtained using the closed-reflux colorimetric method [20] with a HACH DR-700 colorimeter.

H_2O_2 consumption was measured using the KI titration method [21]. Residual H_2O_2 was removed with sulphite [22]. Any remaining sulphite was removed by bubbling O_2.

3. Results and discussion

3.1 Preliminary runs

The performance of Fenton's reagent is associated to different variables, namely the pH, the temperature and the initial H_2O_2 and Fe (II) dosage. In consequence, a lot of measurements would be necessary if these four variables were considered in the experimental design. However, if the role of these variables were previously known, it would be possible to simplify the experimental analysis.

3.1.1 Effect of the initial pH

It is well known that the performance of such a complex reactive system depends on the medium's pH [7], with a maximum catalytic activity a pH around 3 [23-26]. For higher pH values this catalytic activity decreases, due to formation and precipitation of $Fe(OH)_3$, formation of different complex species and break down of H_2O_2 to O_2 and H_2O. However, accepting that different samples could give best performance at different pH values, we performed experiments at pH values between 2.0 and 4.0, in

order to find the best pH to treat our dye solution. Temperature was maintained at 298 K and treatment time was 60 min. The initial H_2O_2 and Fe (II) dosages in these preliminary experiments were 350 $mg \cdot L^{-1}$ (10.3 mM) and 60 $mg \cdot L^{-1}$ (1.07 mM), respectively. This means a molar ratio H_2O_2/Fe(II) of approximately 10. These concentrations were selected according technical literature and stoichiometric requirements for COD reduction [24]. The initial COD for 250 $mg \cdot L^{-1}$ CI Reactive Yellow 145 dye was 172 $mg \cdot L^{-1}$ O_2.

From results showed in Figure 2, we could state that maximum COD reduction was obtained at a pH between 2.5 and 3.0. As said before, for higher pH values, ferric oxyhydroxides precipitation took place with the consequent decrease of Fe^{2+} species [27]. For pH's below 3 the activity decrease was associated to the inhibition of complexation of Fe (III) with H_2O_2 and the photoactivity of Fe (II) species present in solution. Under such conditions [28]:

$$Fe^{3+} + H_2O_2 \rightarrow Fe^{2+} + H^+ + HO\cdot_2 \quad (7)$$

Consequently, from this point we performed all experiments at pH=3.

3.2 Experimental design

In this study, after the exploratory runs, to find the optimum conditions for degradation of CI Reactive Yellow 145 dye under Fenton's and photo-Fenton's conditions, we selected a central composite design (CCD), due to the responses could be simply related

to the chosen factor (% COD reduction in our case) using linear or quadratic models. CCD is a widely used form of RSM. RSM could be considered as a particular set of mathematical and statistical tools for designing experiments, building models, evaluating the effects of operating conditions and researching optimal values of factors to predict target responses [29]. A second-order polynomial response equation was used to attain interaction between dependent and independent variables.

$$Y = b_0 + b_1X_1 + b_2X_2 + b_3X_3 + b_{12}X_1X_2 + b_{13}X_1X_3 + b_{23}X_2X_3 + b_{11}X_1^2 + b_{22}X_2^2 + b_{33}X_3^2 \quad (8)$$

where, Y corresponds to the response variable of % COD reduction; X_i represent the three independent variables selected for the experimental design; b_i values represent regression coefficients for linear effects; b_{ii} the regression coefficients for squared effects and b_{ik} the regression coefficients for interaction effects.

The total number of experiments for the three level CCD employed was 17. Temperature (X_1), the H_2O_2 concentration (X_2) and the Fe(II) concentration (X_3) were the independent variables. The low, centre and high levels that defined the range of each variable were designated as -1, 0 and +1 respectively, (Table 1). Also, the CCD used, required that experiments outside the experimental range previously defined should be performed to allow the prediction of the response functions outside the cubic domain (denoted as ± 1.68; Table 1) [30]. In summary, among the 17 experiments performed, 8 correspond to the factorial design, 6 to the expansions and 3 were carried out in the centre of the cubic domain and a 95% confidence level.

We considered the following ranges in the values of the working variables in the experimental design method: (i) reaction temperatures, T (K) = [298; 318]; (ii) H_2O_2 concentration (mM) = [5.88; 17.65]; and (iii) Fe(II) concentration (mM) = [0.36; 1.79].

The operating range of temperature was chosen to give a variation high enough in terms of practical interest and taking into account the fact that higher temperatures could lead to H_2O_2 decomposition and the loss of iron by precipitation [31]. For the other two variables, the low and high levels for H_2O_2 and Fe (II) were chosen based on technical literature, stoichiometric requirements [24] and on the fact that too high iron and peroxide concentrations could affect negatively to degradation of the process [32].

In table 2 it can be seen the results of the different treatment combinations under dark Fenton and photo-Fenton conditions at pH = 3 and t = 60 min. treatment. As said before, three of the experiments were conducted at the central points, in order to check reproducibility and evaluate the errors. For these runs (runs 15-17), COD reduction ranged from 77.4 and 78.1 % in the case of dark Fenton treatment, and 87.5 and 88.1 % in photo-Fenton treatment.

A Modde software (Umetrics) was used to obtain a quadratic model that gave us an empirical relationship between the % COD reduction (*Y)* and the three independent factors (X_1 *(T)*, X_2 *([H_2O_2])* and X_3 *([Fe (II)])*):

$$Y_1 \text{ (\%COD reduction, after 60 min. Fenton treatment)} = 78.32\ (\pm 11.09) - 1.72\ (\pm 5.21)X_1 + 5.79(\pm 5.21)X_2 + 14.25(\pm 5.21)X_3 - 5.55(\pm 5.73)X_1^2 - 13.13(\pm 5.73)X_2^2 - 20.01(\pm 5.73)X_3^2 + 0.05(\pm 6.80)X_1 \cdot X_2 - 0.275(\pm 6.80)X_1 \cdot X_3 + 2.425(\pm 6.80)X_2 \cdot X_3 \quad (9)$$

Y_2 *(% COD reduction, after 60 min. photo-Fenton treatment)* = 88.34 (±9.93) -1.63 (±4.66)X_1 + 6.53(±4.66)X_2 + 15.64(±4.66)X_3 -6.75(±5.13)X_1^2 -14.19(±5.13)X_2^2 -22.16 (±5.13)X_3^2 +0.20(±6.09)$X_1 \cdot X_2$ -0.325(±6.09)$X_1 \cdot X_3$ +3.175(±6.09)$X_2 \cdot X_3$ (10)

The COD reduction efficiencies have been predicted by equations (9) and (10) and presented in Table 3. These results indicated good agreements between experimental and predicted values for COD reduction.

Next, adequacy of the models was justified through analysis of variance (ANOVA). The ANOVA for the quadratic model for % COD reduction, under Fenton and photo-Fenton conditions, could be seen in Table 4. In the ANOVA test, the F-ratio value obtained for the percentage of COD reduction is higher than the Fisher's F-value ($F_{9,7}$ = 3.80). Consequently, we could say that the model was significant for dye COD reduction. The quality of the fit of the polynomial model was expressed by the determination coefficient R^2. From R^2 = 0.948 in Fenton treatment and R^2 = 0.965 in photo-Fenton treatment, we could say that 94.8 % and 96.5% of the response variability was explained by the model and the model did not explain only 5.2 and 3.5 % of variation respectively. From these values, we could state that a good correlation was obtained, indicating a good fit by the model, for which the criterion of R^2 at least 0.80 is suggested [14].

Subsequently, the statistically significant variables and/or interactions were identified, using the Student's *t*-test. The obtained results could be seen in Table 5. From these results we could say that H_2O_2 (X_2) and Fe (II) (X_3) concentrations were significant model terms and had a positive effect on the response (P values smaller than 0.05 for 95

% confidence level). Fe (II) concentration had a stronger effect than H_2O_2 concentration. On the other hand, temperature was negligible compared to the other variables, according to the fact that this variable was only important in the first stages of the Fenton reactions [33]. A positive effect of a variable, mean that the % COD reduction was improved when the variable level increased. A negative effect means that the response was not improved when the factor level was increased.

In order to visualize the relationship between experimental variables and responses, response surface and contour plots were generated from the model. A study of the response surface and contour plots provided an interesting method for the optimization of Fenton's and photo-Fenton's processes. A MODDE software to produce response surface and contour plots was used. In figures 3 and 4, the response surface and contour plots were presented as a function of H_2O_2 and Fe (II) concentrations respectively. Temperature was kept constant at 298 K, given that we found temperature was not a significant variable and did not affect performance of reactions. Also, pH was maintained at 3 according to preliminary runs.

Figures 3 and 4 illustrated the effect of Fe (II) and H_2O_2 concentrations on % COD reduction. It could be concluded that the most important parameter for the reduction of COD, was the Fe(II) concentration. H_2O_2 also was a significant variable, but affected removal efficiency in a lower extent. H_2O_2 and Fe (II) concentrations affected positively the COD reduction. As it is obvious from Figures 3 and 4, chemical oxygen demand efficiency increased with increasing Fe (II) and H_2O_2 concentrations. However, when one moved towards higher Fe (II) or H_2O_2 concentrations, a detrimental effect in COD reduction could be seen. The detrimental effect could be related with the scavenging of radicals, as it is shown in the following equations (11-13):

$H_2O_2 + HO\cdot \rightarrow HO\cdot_2 + H_2O$ (11)

$Fe(II) + HO\cdot \rightarrow Fe(III) + OH^-$ (12)

$Fe(II) + HO_2\cdot \rightarrow Fe(III) + HO_2^-$ (13)

However, a significant Fe(II) concentration was needed in order to produce Fenton's reactions. When the lowest Fe (II) level was used ([Fe (II)] = 0 (measure 13)), the worst results were obtained.

From these plots and the aforementioned comments, optimum results for the COD reduction, were obtained under the following optimal conditions: pH =3; T = 298 K; [Fe(II)] = 1.075 mM and $[H_2O_2]$ = 11.765 mM. In this case the molar ratio used was H_2O_2/Fe(II) = 10.9. Under these optimum conditions, an additional experiment was performed. The obtained results were shown in Figure 5. A 79 % decrease in COD under Fenton treatment and 92.2% decrease under photo-Fenton treatment were obtained. This Figure showed that in the first minutes of reaction, the COD decrease in dark Fenton and photo-Fenton treatments was similar. This fact could be explained by considering that the initial COD decrease was mainly due to dark Fenton reaction, which is faster than photo-Fenton reactions [26]. For long reaction times, obtained results were different from both treatments. UVA radiation improved COD reduction. Light could play two different roles that will lead to an improvement of the reaction yields: (a) it drives photo-Fenton reaction, producing extra hydroxyl radicals and the

regeneration of Fe (II) needed in Fenton reaction, as indicated in reaction (6). The photo-Fenton reaction may involve direct photolysis of ferric ion or photolysis of Fe(III)-peroxy complexes or any of their potential intermediates. (b) It can drive ligand to metal charge transfer in the potentially photolabile complexes formed by Fe (III) and the carboxylic acid moiety [34].

At this point, the level of residual H_2O_2 was determined, because it is a key parameter in determining the optimal H_2O_2 concentration when Fenton's processes are employed as a treatment or a step connected to a biological treatment. Figure 6 showed the evolution of the H_2O_2 concentration under optimal conditions for the dark Fenton and photo-Fenton reactions. As it could be seen, a 400 $mg \cdot L^{-1}$ H_2O_2 concentration (11.765 mM) supplied the needed oxidant to degrade the dye and the remaining H_2O_2 after 60 min. treatment was very low.

4. Conclusions

According to experimental results, a quadratic polynomial was obtained for our response (% COD reduction), under Fenton's and photo-Fenton's conditions. The optimization procedure produced high and significant R^2 and R^2_{adj} values for both treatments. Consequently we could assure a good adjustment of the quadratic regression model with the experimental data. These values were: 0.948 and 0.882 for Fenton treatment and 0.965 and 0.921 in the case of photo-Fenton treatment.

Among the studied variables, it could be seen that the largest effect in COD reduction efficiency was due to Fe (II) concentration. Also, our preliminary analysis demonstrated

that pH should be maintained at 3 and reaction could be carried out efficiently at room temperature. To summarize, the optimal reaction conditions were thus pH =3; T = 298 K; [Fe (II)] = 1.075 mM and [H_2O_2] = 11.765 mM. Under these conditions and with a 60-min treatment, a 79% and 92.2% COD decrease under Fenton and photo-Fenton treatments, respectively, was obtained.

Moreover, this study showed that RSM was an appropriate technique to optimize the operating conditions and maximize dye removal.

References

[1] P. Grau, Textile industry wastewaters treatment, Water Sci. Technol. 24 (1991), pp. 97-103.

[2] C.O'Neil, F.R. Hawkes, D.I. Hawkes, N.D. Lourenço, H.M. Pinheiro, W.Delée, Colour in textile effluents-sources, measurement, discharge consents and simulation: a review, J.Chem. Technol. Biotechnol. 74 (11) (1999), pp. 1009-1018.

[3] A. Uygur, E. Kök, Decolorisation treatments of azo dyes wastewaters including dichlorotriazinyl reactive groups by using advanced oxidation method, J. Soc. Dyers Colour. 115 (1999), pp. 350-354.

[4] YM. Slokar, A. Majcen Le Marechal, Methods for decolorization textile wastewatrers, Dyes Pigments 37 (1998), pp. 335-336.

[5] S. Chakraborty, S. De, J.K. Basu, S. DasGupta, Treatment of a textile effluent: application of a combination method involving adsorption and nanofiltration, Desalination 174 (2005), pp. 73-85.

[6] O. Türgay, G. Ersöz, S. Atalay, J. Forss, U. Welander, The treatment of azo dyes found in textile industry wastewater by anaerobic biological method and chemical oxidation, Sep.Purif.Technol. 79 (2011), pp. 26-33.

[7] J. Pignatello, E. Oliveros, A. MacKay, Advanced oxidation processes for organic contaminant destruction based on the Fenton reaction and related chemistry, Crit. Rev. Environ. Sci. Technol. 36 (2006), pp. 1-84.

[8] B. Lodha, S. Chaudhari, Optimization of Fenton-biological treatment scheme for the treatment of aqueous dye solutions, J. Hazard. Mater. 148 (2007), pp. 459-466.

[9] N.K. Daud, U.G. Akpan and B.H. Hameed, Decolorization of Sunzol Black DN conc. in aqueous solution by Fenton oxidation process: effect of system parameters and kinetic study, Desalin. Water Treat. 37 (2012), pp. 1-7.

[10] A. Aris, P.N. Sharrat, Fenton oxidation of reactive black 5: Effect of mixing intensity and reagent addition strategy, Environ. Technol. 25 (5) (2004), pp. 601-612.

[11] M. Muruganandham, M. Swaminathan, Decolorisation of Reactive Orange 4 by Fenton and photo-Fenton oxidation technology, Dyes Pigments 63 (2004), pp. 315-321.

[12] J. García-Montaño, F. Torrades, L.A. Pérez-Estrada, I. Oller, S. Malato, M.I. Maldonado, J.Peral, Degradation pathways of the commercial reactive azo dye Procion Red H-E7B under solar-assisted photo-Fenton reaction, Environ. Sci. Technol. 42 (2008), pp. 6663-6670.

[13] S. Vilhunen, M. Sillanpää, Recent developments in photochemical and chemical AOPs in water treatment: a mini-review, Rev. Environ. Sci. Biotechnol. 9 (2010), pp. 323-330.

[14] S.L.C. Ferreira, R.E. Bruns, H.S. Ferreira, G.D. Matos, et.al., Box-Behnken design: an alternative for the optimization of analytical methods, Anal. Chim. Acta 597 (2007), pp. 179-186.

[15] I. Arslan-Alaton, G. Tureli and T. Olmez-Hanci, Optimization of the photo-Fenton-like process for real synthetic azo dye production wastewater treatment using response surface methodology, Photochem. Photobiol. Sci. 8 (2009), pp. 628-638.

[16] A.R. Khtaee, M. Zarei, M. Fathinia, M. Khobnasab Jafari, Photocatalytic degradation of an anthraquinone dye on immobilized TiO_2 nanoparticles in a rectangular reactor. Destruction pathway and response surface approach, Desalination 268 (2011), pp. 126-133.

[17] Diya'udeen Basher Hasan, A.R. Abdul Aziz, Wan Mohd Ashri Wan Daud, Using D-optimal experimental design to optimize remazol black B mineralization by Fenton-like peroxidation, Envion. Technol. 33 (10) (2012), pp. 1111-1121.

[18] F. Ay, E. Cocay Catalkaya, F. Kargi, Advanced Oxidation of Direct red (DR 28) by Fenton treatment, Environ. Eng. Sci. 25 (2008), pp. 1455-1462.

[19] F. Ay, E. Cocay Catalkaya, F. Kargi, A statistical experiment design approach for advanced oxidation of Direct Red azo-dye by photo-Fenton treatment, J. Hazard. Mater. 162 (2009), pp. 230-236.

[20] APHA-AWWA-WPCF, Standard Methods for the Examination of Water and Wastewater, (1989). ASTM D1252-00, 17th ed., APHA-AWWA-WPCF, Washington, DC.

[21] C. Kormann, D.W. Bahnemann, M.R. Hoffmann, Photocatalytic production of hydrogen peroxides and organic peroxides in aqueous suspensions of titanium dioxide, zinc oxide and desert sand, Environ. Sci. Technol. 22 (1988), pp. 798-806.

[22] CD. Adams, PA Scanlan, ND Secrist, Oxidation and biodegradability enhancement of 1,4-dioxane using hydrogen peroxide and ozone, Environ. Sci. Technol. 28 (1994), pp. 1812-1818.

[23] R. Bauer, H. Fallman, The photo-Fenton oxidation-a cheap and efficient wastewater treatment method, Res. Chem. Intermed. 23 (1997), pp. 341-354.

[24] N.H. Ince, G. Tezcanli, Treatability of texyile dye-bath effluents by advanced oxidation: Preparation for reuse, Water Sci. Technol. 40 (1999), pp. 183-190.

[25] R.F.P. Nogueira, J.R. Guimaraes, Photodegradation of dichloroacetic acid and 2,4-dichlorophenol by ferrioxalate/H_2O_2 system, Water Res. 34 (2000), pp. 895-901.

[26] F.Torrades, J.A. García-Hortal, L. Núñez, Fenton and photo-Fenton oxidation of a model mixture of dyes –overall kinetic analysis, Color. Technol. 124 (2008), pp. 370-374.

[27] R. Oliveira, M.F. Almeida, L. Santos, L. M. Madeira, Experimental design of 2,4-dichlorophenol oxidation by Fenton's reaction, Ind. Eng. Chem. Res. 45 (2006), pp. 1266-1276.

[28] M.S. Lucas, J.A. Peres, Decolorization of the azo dye reactive Black 5 by Fenton and photo-Fenton oxidation, Dyes Pigments 71 (2006), pp. 236-244.

[29] K. Cruz-Gonzales, O. Torres-López, A. García-León, J.L. Guzmán-Mar, L.H. Reyes, A. Hernández-Ramirez, J.M. Peralta-Hernández, Determination of optimum operating parameters for Acid Yellow 36 decolorization by electro-Fenton process using BDD cathode, Chem. Eng. J. 160 (2010), pp. 199-206

[30] F. Torrades, S. Saiz, J.A. García-Hortal, Using central composite experimental design to optimize the degradation of black liquor by Fenton reagent, Desalination 268 (2011), pp. 97-102.

[31] A. Zapata, I. Oller, E.Bizani, J.A. Sánchez-Pérez, M.I. Maldonado, S. Malato, Evaluation of operational parameters involved in solar photo-Fenton degradation of a comercial pesticide mixture, Catal. Today 144 (2009), pp. 94-99.

[32] S.H. Lin, C.C. Lo, Fenton process for treatment of desizing wastewater, Water Res. 31 (1997), pp. 2050-2056.

[33] F.Torrades, J. García-Montaño, J.A. García-Hortal, L. Núñez, X. Domènech and J.Peral, Decolorisation and mineralisation of homo- and hetero-bireactive dyes under Fenton and photo-Fenton conditions, Color. Technol. 120 (2004), pp. 188-194.

[34] M. Pérez, F. Torrades, J.A. García-Hortal, X. Domènech, J. Peral, Removal of organic contaminants in paper pulp effluents under Fenton and photo-Fenton conditions, Appl. Catal. B: Environ. 36 (1) (2002), pp. 63-74.

Tables

Table 1.- Levels of the parameters studied in CCD statistical experiment

Table 2.- Central Composite design matrix. Response factor results (%COD reduction, after Fenton and photo-Fenton treatments)

Table 3.- Predicted and experimentally achieved removal efficiencies for each run

Table 4.- ANOVA results for % COD reduction under Fenton and photo-Fenton treatments

Table 5.- Estimates of the model regression for % COD reduction under Fenton and photo-Fenton treatments

Figure captions

Fig.1 Chemical structure of Sumifix Supra Yellow 3RF (CI Reactive Yellow 145)

Fig. 2 Effect of initial pH on the COD removal from CI Reactive Yellow 145 dye, for a treatment time of 60 min., $[H_2O_2]$ = 10.8 mM, [Fe(II)] = 1.08 mM and T = 298 K.

Fig. 3 The response surface plot and contour plot of the chemical oxygen demand efficiency (% COD reduction), from CI Reactive Yellow 145 dye after 60 min. Fenton treatment, as a function of $[H_2O_2]$ and [Fe(II)] at T = 298 K and pH =3.

Fig. 4 The response surface plot and contour plot of the chemical oxygen demand efficiency (% COD reduction), from CI Reactive Yellow 145 dye after 60 min. photo-Fenton treatment, as a function of $[H_2O_2]$ and [Fe(II)] at T = 298 K and pH =3.

Fig. 5 Evolution of COD reduction under optimal conditions (T = 298 K, pH =3, $[H_2O_2]$ = 11.765. mM and [Fe(II)] = 1.075 mM), for Fenton and photo-Fenton treatments.

Fig. 6 Residual H_2O_2 level as a function of time for CI Reactive Yellow 145 dye, under optimal conditions for the dark Fenton and photo-Fenton reactions (T = 298 K, pH =3, initial $[H_2O_2]$ = 11.765 mM and [Fe(II)] = 1.075 mM).

Table 1

Variable	**Coded Variable**				
	-1.68	**-1**	**0**	**+1**	**+1.68**
T (K)	291.2	298	308	318	324.8
[H_2O_2]/(mM)	1.87	5.88	11.765	17.65	21.66
[Fe(II)]/(mM)	0.00	0.36	1.075	1.79	2.28

Table 2

				% reduction	**% reduction**
Run No.	T(K)	H_2O_2/(mM)	Fe (II)/(mM)	COD (Fenton)	COD (photo-Fenton)
1	-1 (298)	-1 (5.88)	-1 (0.36)	15.2	20.1
2	+1 (318)	-1 (5.88)	-1 (0.36)	15.9	21.2
3	-1 (298)	+1 (17.65)	-1 (0.36)	26.2	31.4
4	+1 (318)	+1 (17.65)	-1 (0.36)	27.1	32.6
5	-1 (298)	-1 (5.88)	+1 (1.79)	40.2	46.3
6	+1 (318)	-1 (5.88)	+1 (1.79)	39.8	45.4
7	-1 (298)	+1 (17.65)	+1 (1.79)	60.9	69.6
8	+1 (318)	+1 (17.65)	+1 (1.79)	60.7	70.2
9	-1.68 (291.2)	0 (11.765)	0 (1.075)	75.4	80.9
10	+1.68 (324.8)	0 (11.765)	0 (1.075)	60.8	66.5
11	0 (308)	-1.68 (1.866)	0 (1.075)	42.1	47.2
12	0 (308)	+1.68 (21.66)	0 (1.075)	51.2	58.1
13	0 (308)	0 (11.765)	-1.68 (0.00)	4.2	4.1
14	0 (308)	0 (11.765)	+1.68 (2.28)	50.2	56.1
15	0 (308)	0 (11.765)	0 (1.075)	77.4	88.1
16	0 (308)	0 (11.765)	0 (1.075)	77.6	87.5
17	0 (308)	0 (11.765)	0 (1.075)	78.1	87.9

Table 3

% COD removal (Fenton)			% COD removal (photo-Fenton)		
Run No.	Actual	Predicted	Run No.	Actual	Predicted
1	15.2	23.5	1	20.1	27.7
2	15.9	20.5	2	21.2	24.7
3	26.2	30.1	3	31.4	34.1
4	27.1	27.4	4	32.6	31.9
5	40.2	47.7	5	46.3	53.3
6	39.8	43.6	6	45.4	49.0
7	60.9	64.0	7	69.6	72.3
8	60.7	60.1	8	70.2	68.8
9	75.4	65.5	9	80.9	72.0
10	60.8	59.7	10	66.5	66.5
11	42.1	31.4	11	47.2	37.2
12	51.2	50.9	12	58.1	59.2
13	4.2	0.0	13	4.1	0.0
14	50.2	45.7	14	56.1	52.0
15	77.4	78.3	15	88.1	88.3
16	77.6	78.3	16	87.5	88.3
17	78.1	78.3	17	87.9	88.3

Table 4

	Source	df	SS	MS	F-ratio	P-value
Fenton	Model	9	8530.1	947.8	14.31	0.001
	Residual	7	463.5	66.2		
	Total	16	8993.6	562.1		
	$R^2 = 0.948$ $R^2_{adj.} = 0.882$					
Photo-Fenton	Model	9	10331.3	1147.9	21.67	0.000
	Residual	7	371.8	53.1		
	Total	16	10703.1	668.94		
	$R^2 = 0.965$ $R^2_{adj.} = 0.921$					

Table 5

	Term	Estimate	Standard error	*t*-value	P-value
Fenton	Intercept	78.32	4.69	16.70	0.000
	T	-1.72	2.20	-0.78	0.459
	$[H_2O_2]$	5.79	2.20	2.63	0.034
	[Fe(II)]	14.25	2.20	6.48	0.000
	$T \cdot [H_2O_2]$	0.05	2.88	0.02	0.987
	T·[Fe(II)]	-0.275	2.88	-0.09	0.926
	$[H_2O_2] \cdot [Fe(II)]$	2.425	2.88	0.84	0.427
	T^2	-5.55	2.42	-2.29	0.056
	$[H_2O_2]^2$	-13.13	2.42	5.43	0.001
	$[Fe(II)]^2$	-20.01	2.42	-8.27	0.000
Photo-Fenton	Intercept	88.34	4.20	21.03	0.000
	T	-1.63	1.97	-0.83	0.437
	$[H_2O_2]$	6.53	1.97	3.31	0.013
	[Fe(II)]	15.64	1.97	7.94	0.000
	$T \cdot [H_2O_2]$	0.20	2.58	0.08	0.940
	T·[Fe(II)]	-0.325	2.58	0.13	0.903
	$[H_2O_2] \cdot [Fe(II)]$	3.175	2.58	1.23	0.258
	T^2	-6.75	2.17	-3.11	0.017
	$[H_2O_2]^2$	-14.19	2.17	-6.54	0.000
	$[Fe(II)]^2$	-22.16	2.17	-10.21	0.000

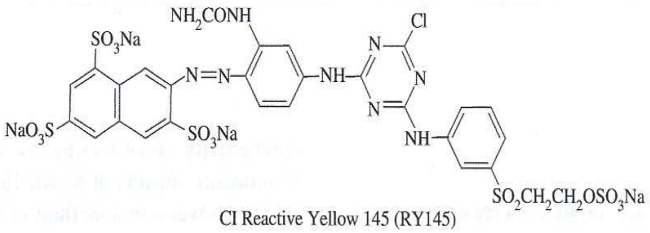

CI Reactive Yellow 145 (RY145)

Figure 1

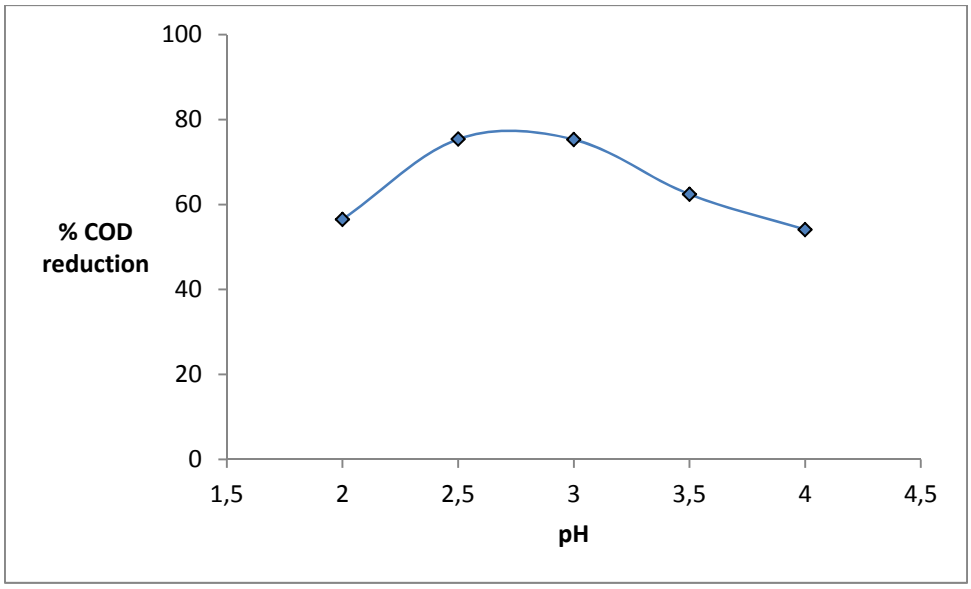

Figure 2

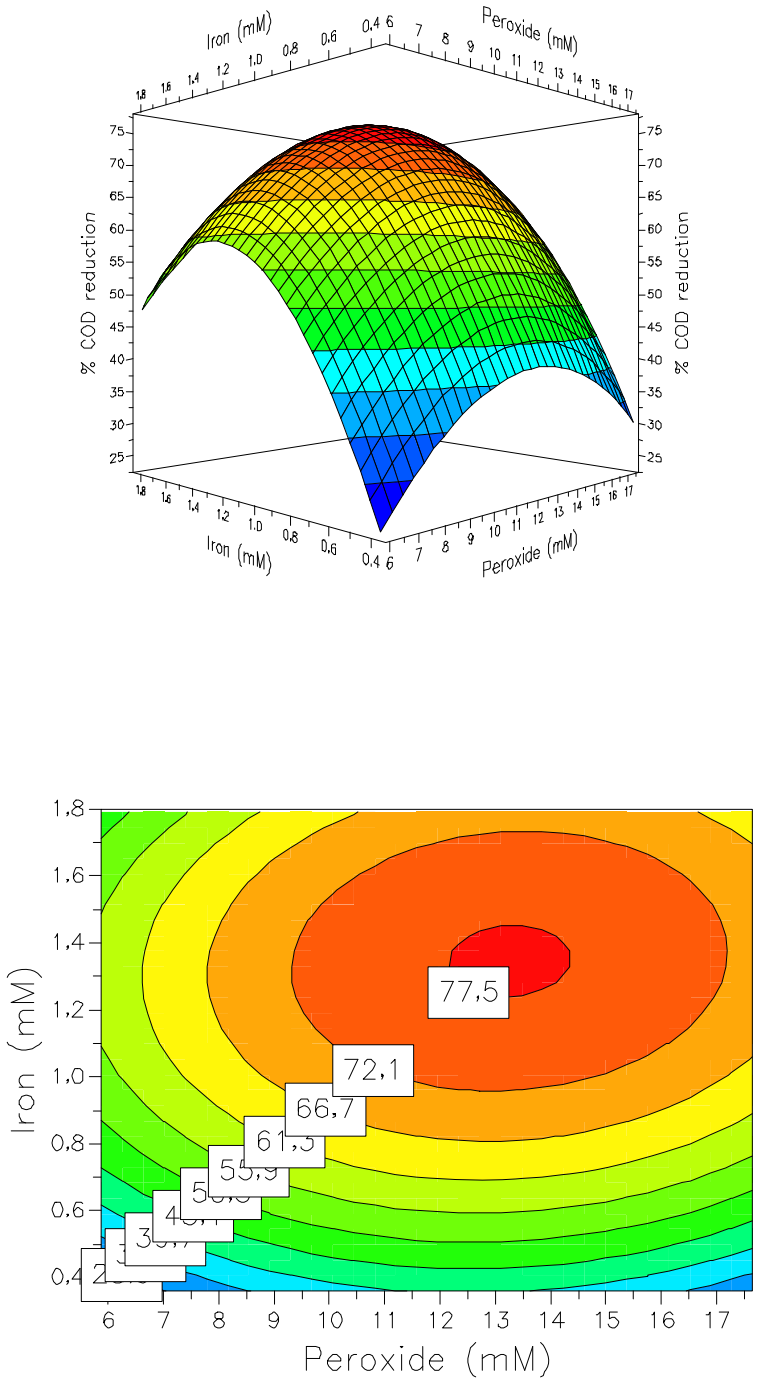
Iron (mM)
Peroxide (mM)
% COD reduction
% COD reduction
Iron (mM)
Peroxide (mM)
77,5
72,1
66,7
Iron (mM)
Peroxide (mM)

Figure 3

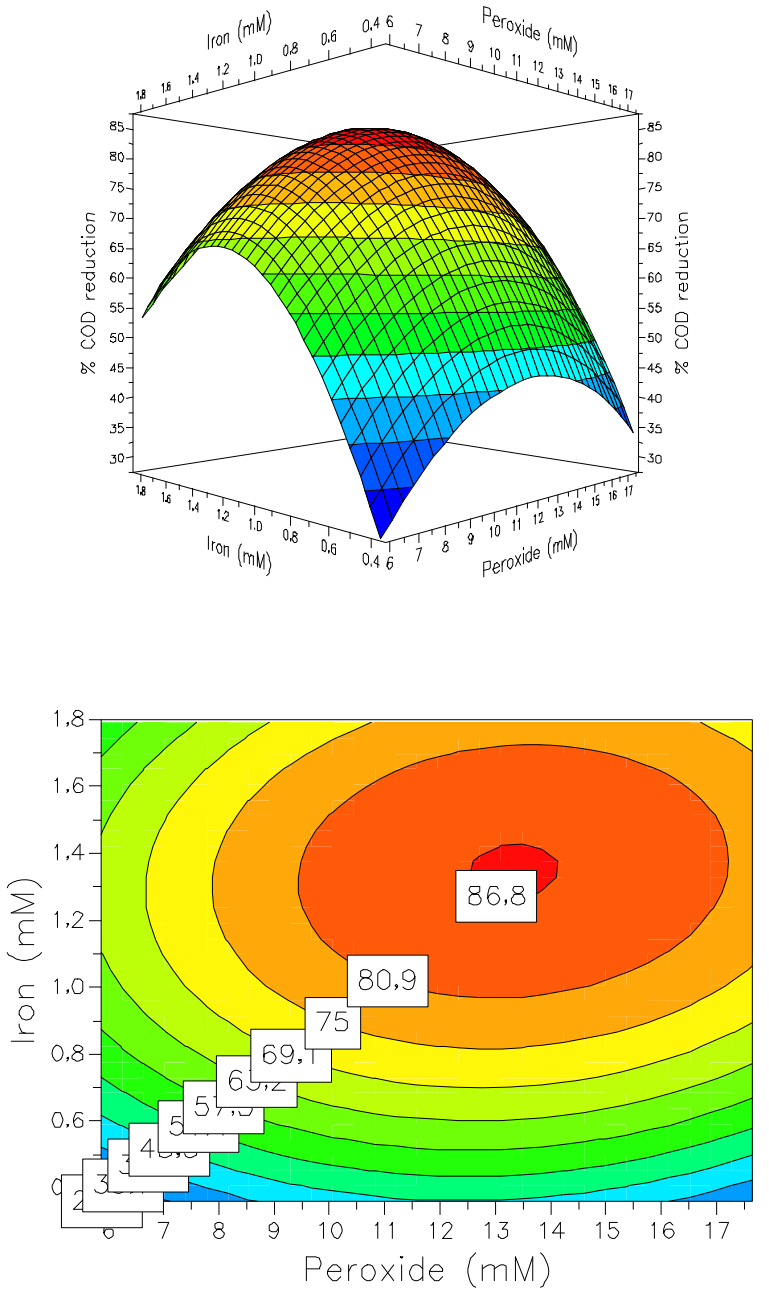
Iron (mM)
Peroxide (mM)
% COD reduction
% COD reduction
Iron (mM)
Peroxide (mM)
Iron (mM)
Peroxide (mM)
86,8
80,9
75

Figure 4

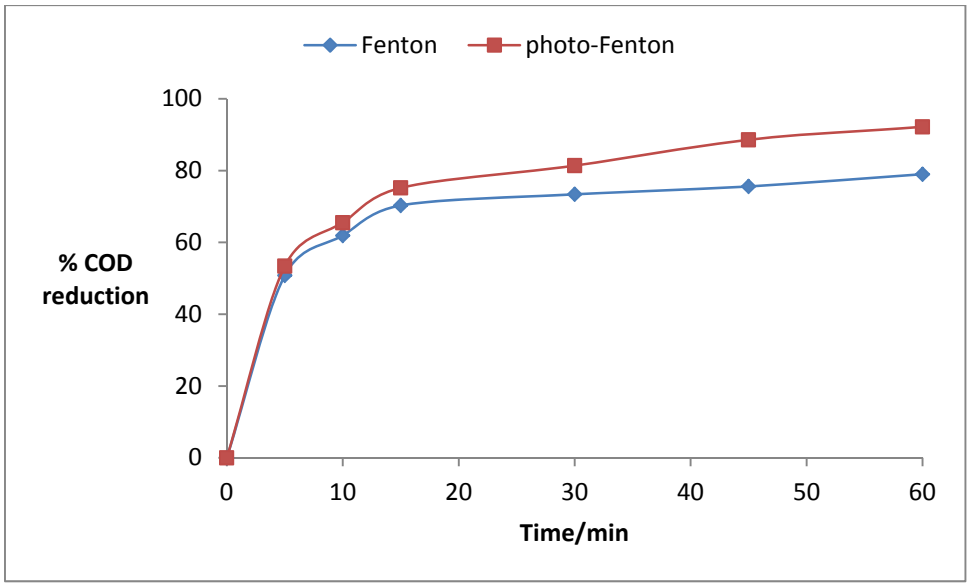
Fenton
photo-Fenton
100
80
60
40
20
0
% COD reduction
0
10
20
30
40
50
60
Time/min

Figure 5

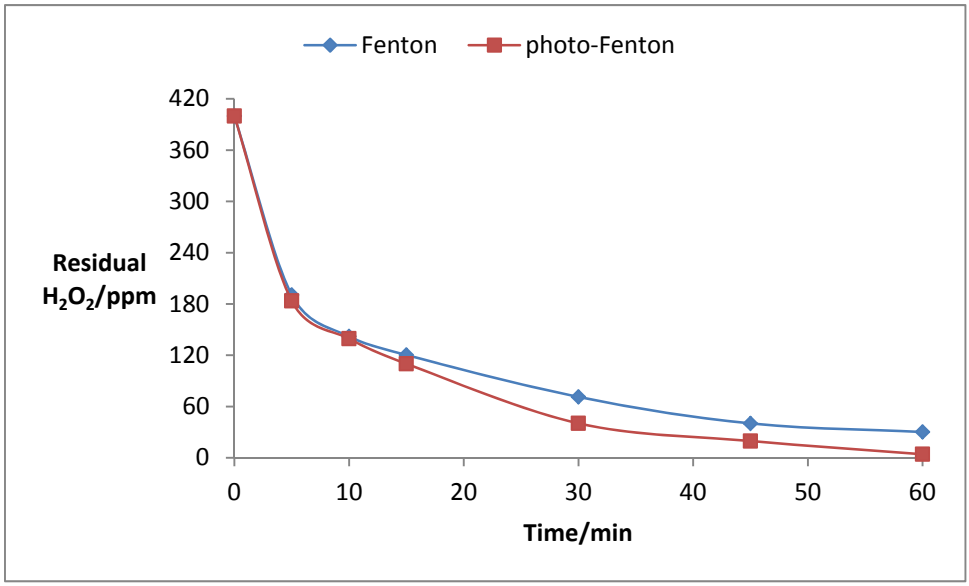
Fenton
photo-Fenton
Residual
H2O2/ppm
420
360
300
240
180
120
60
0
0
10
20
30
40
50
60
Time/min

Figure 6